Title

Poly (Ethylene Glycol)-Based Hydrogels as Self-Inflating Tissue Expanders with Tunable Mechanical and Swelling Properties

Journal

Macromolecular Bioscience, 17(8)

ISSN

1616-5187

Authors

Jamadi, Mahsa
Shokrollahi, Parvin
Houshmand, Behzad
et al.

Publication Date

2017-08-01

DOI

10.1002/mabi.201600479

Peer reviewed

Poly (Ethylene Glycol)-Based Hydrogels as Self-Inflating Tissue Expanders with Tunable Mechanical and Swelling Properties

Mahsa Jamadi, Parvin Shokrollahi,* Behzad Houshmand,* Mortaza Daliri Joupari, Fatemeh Mashhadiabbas, Ali Khademhosseini, Nasim Annabi

Tissue expansion is used by plastic/reconstructive surgeons to grow additional skin/tissue for replacing or repairing lost or damaged soft tissues. Recently, hydrogels have been widely used for tissue expansion applications. Herein, a self-inflating tissue expander blend composition from three different molecular weights (2, 6, and 10 kDa) of poly (ethylene glycol) diacrylate (PEGDA) hydrogel with tunable mechanical and swelling properties is presented. The in vitro results demonstrate that, of the eight studied compositions, P6 (PEGDA 6 kDa:10 kDa (50:50)) and P8 (PEGDA 6 kDa:10 kDa (35:65)) formulations provide a balance of mechanical property and swelling capability suitable for tissue expansion. Furthermore, these expanders can be compressed up to 60% of their original height and can be loaded and unloaded cyclically at least ten times with no permanent deformation. The in vivo results indicate that these two engineered blend compositions are capable to generate a swelling pressure sufficient to dilate the surrounding tissue while retaining their original shape. The histological analyses reveal the formation of fibrous capsule at the interface between the implant and the subcutaneous tissue with no signs of inflammation. Ultimately, controlling the PEGDA chain length shows potential for the development of self-inflating tissue expanders with tunable mechanical and swelling properties.

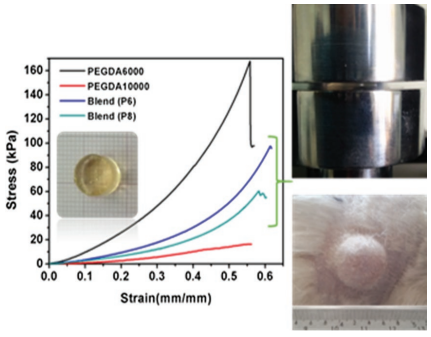

M. Jamadi, Prof. A. Khademhosseini, Prof. N. Annabi
Biomaterials Innovation Research Center
Division of Biomedical Engineering
Department of Medicine
Brigham and Women's Hospital
Harvard Medical School
Cambridge, MA 02139, USA
M. Jamadi, Prof. A. Khademhosseini, Prof. N. Annabi
Harvard-MIT Division of Health Sciences and Technology
Massachusetts Institute of Technology
Cambridge, MA 02139, USA
M. Jamadi, Prof. B. Houshmand (Visiting Professor)
Stem Cell and Regenerative Medicine Division
National Institute of Genetic Engineering and Biotechnology
Tehran 14977-16316, Iran
E-mail: houshmandperio@rocketmail.com

Dr. P. Shokrollahi
Department of Biomaterials
Iran Polymer and Petrochemical Institute
Tehran 14977-13115, Iran
E-mail: p.shokrolahi@ippi.ac.ir
Prof. B. Houshmand
Department of Periodontics
School of Dentistry
Shahid Beheshti University of Medical Sciences
Tehran 19839-69411, Iran
Dr. M. D. Joupari
Animal Biotechnology Department
National Institute of Genetic Engineering and Biotechnology,
Tehran 14977-16316, Iran

DOI: 10.1002/mabi.201600479

1. Introduction

Shortage of available soft tissues is a common challenge in reconstructive surgeries.[1] The use of soft tissue expanders can overcome some of the challenges. A tissue expander is known as a device especially designed to induce skin or tissue expansion in response to stress or to a given deformation for reconstructive/plastic surgeries.[2] Keeping a tissue under constant tension may be resulted in skin stretching,[3] which may change the extracellular matrix (ECM) organization and stimulate cell division, resulting in the formation of new tissues.[4] Enlargement of soft tissue volume as well as its superficial area is a natural phenomenon, observed in obesity and pregnancy.[1] Soft tissue expansion is now a widely used reconstructive technique with a variety of applications, including correction of burn alopecia of the scalp and postmastectomy breast reconstruction.[5]

The use of tissue expansion in reconstructive plastic surgery was introduced by Neumann in 1957, and later on popularized by Radovan[6,7] and Argenta et al.[8] Conventional tissue expanders are based on a silicone balloon, which is introduced into the target area and then gradually inflated by injection of sterile saline solution over a pre-determined period of time.[9] However, this technique involves the risks of various complications and inconveniences, such as increasing pressure in the balloon, inducing necrosis and perforation. Other complications associated with this approach include leakage, migration, flap necrosis, infection and wound separation.[10] Furthermore, regular control is needed, which is time consuming and expensive[11] and can be poorly tolerated by the patient, specifically in the pediatric setting.[9] In addition, physical restrictions of the device may prevent its use in some anatomical locations (e.g., craniofacial or cleft palate surgery).[9] Hence, development of a new generation of tissue expanders may be useful in order to eliminate these limitations.[11]

To address these shortcomings, the first self-inflating tissue expander, made of a silicone membrane filled with a hypertonic saline solution, was introduced.[12] In this system, tissue expansion was triggered by swelling of osmotically driven water uptake of subcutaneously implanted tissue expanders.[12] However, full expansion of the silicone balloon in this system required an extended time (8–14 weeks) and induced tissue necrosis.[13]

To overcome these limitations, the use of hydrogels as tissue expander instead of silicone membrane has been investigated.[9] Hydrogels' expansion is based on their ability to absorb and retain large volume of water or physiological fluid[14] which is determined by the compositions of the hydrogels.[15] In order to promote tissue expansion, a hydrogel must withstand mechanical loading from the surrounding soft tissues or the skin.[2] However, the low mechanical properties of swollen hydrogels are the main disadvantage of using gels as tissue expanders.[16–18] Elastic hydrogels are known to be resilient to compression and elongation after swelling.[2] Such elastic hydrogels are promising candidates as tissue expanders, with capability of harvesting tissue for reconstructive interventions.[2]

A hydrogel-based tissue expander with osmotic driving force containing polyvinylpyrrolidone and poly (hydroxyethyl methacrylate) was developed for the treatment of congenital anophthalmia.[19] Wiese et al. also introduced a self-filling device that produced higher swelling than vinyl pyrrolidone (VP)/methyl methacrylate (MMA) hydrogels, by replacing the CH_3 groups in the VP/MMA hydrogel chains with COOH groups.[15] Although many types of hydrogel-based tissue expanders have been introduced, most of the clinically available hydrogel-based tissue expanders are still based on VP and MMA copolymers.[20–23] The VP/MMA tissue expanders are glassy and brittle in the dry state and lack sufficient resistance against size changes at the time of implantation.[2] Recently, Kemeny et al. synthesized thermosensitive hydrogels made of *N*-isopropylacrylamide (NIPAAm) as osmotic tissue expanders.[24] Silicate was added to the hydrogel to enhance its elastic properties by increasing the value of storage modulus (G′). However, increasing cell adhesion properties due to the addition of silicate[25] may lead to difficult removal of the implant. Overall, the previous engineered expanders could not provide versatile composition formulations with tunable physical properties (stiffness, elasticity, and swelling) based on the desired clinical applications. Therefore, there is an unmet need for developing elastic and flexible self-inflating

Dr. F. Mashhadiabbas
Department of Oral and Maxillofacial Pathology
School of dentistry
Shahid Beheshti University of Medical Sciences
Tehran 19839-69411, Iran
Prof. A. Khademhosseini
Department of Physics
King Abdulaziz University
Jeddah 21569, Saudi Arabia
Prof. A. Khademhosseini
Department of Bioindustrial Technologies
College of Animal Bioscience and Technology
Konkuk University
Seoul 143-701, Republic of Korea
Dr. N. Annabi
Department of Chemical Engineering
Northeastern University
Boston, MA 02115-5000, USA

tissue expanders with tunable physical properties according to each application.

Poly (ethylene glycol) (PEG) is known as one of the most effective synthetic polymers because of its superior hydrophilicity, biocompatibility, and resistance to protein and cell adhesion.[26–28] In addition, the flexible chain structure of PEG reduces its glass transition temperature.[2] PEG is also poorly immunogenic and nontoxic at molecular weights above 400 Da.[29,30] It is also readily cleared through the kidneys, and is approved by the U.S. Food and Drug Administration (FDA) for internal use.[29] PEG-based hydrogels are highly flexible and/or elastic in nature.[27,31,32] PEG acrylates are the major kind of macromeres for the fabrication of elastic PEG-based gels.[33] For example, Im et al. developed a range of biodegradable PEG/polycaprolactone (PCL) hydrogels with different molecular weights for biomedical applications.[27] They found that PEG/PCL gels were elastic even in the dried state and remained intact after repeated cycles of stretching and bending up to twice their original length.[27] It has been shown that PEG diacrylate (PEGDA) hydrogels have tunable physicomechanical properties.[34,35] For example, their mechanical properties can be tuned by changing the concentration or molecular weight of the polymer; i.e., modulus of elasticity enhances as the polymer concentration increases or the polymer molecular weight decreases.[36] The pore size and swelling ratio of PEGDA can also be tuned.[37] Although the use of PEGDA-based hydrogels has been examined for different biomedical applications, their application as a tissue expander has not yet been reported. Therefore, it would be worthwhile to optimize the physical properties of PEGDA-based hydrogels as tissue expanders.

The aim of this study is to develop a high resilient, self-inflating tissue expander with tunable mechanical and swelling properties. PEGDA polymers with different molecular weights were prepared by esterification reaction of acryloyl chloride (Ac) with PEG diols. The prepared diacrylates and their blends were used to form hydrogels through radical cross-linking reactions. Compared to the hydrogels fabricated from one molecular weight of PEGDA, composite hydrogel made of PEGDA with various molecular weights is expected to provide a more versatile and useful design approach for the formation of hydrogels with tunable properties. We anticipate that utilizing this approach, PEGDA-based hydrogel formulations with elasticity and swelling ratio suitable for generating enough pressure to expand soft tissue can be optimized.

2. Results and Discussion

Eight different PEGDA blends of varying wt% ratios of PEGDA-2k/PEGDA-6k/PEGDA-10k at total polymer concentrations of 15 wt% were used to create the cross-linked constructs needed for the chemical and physical tests (Table 1). All the hydrogels retained their initial shape irrespective of the hydration degree.

Table 1. Formulations of the prepared hydrogels.

Samples	PEGDA 2k concentration [wt%]	PEGDA 6k concentration [wt%]	PEGDA 10k concentration [wt%]
P1	100	0	0
P2	0	100	0
P3	0	0	100
P4	50	50	0
P5	50	0	50
P6	0	50	50
P7	33.3	33.3	33.3
P8	0	35	65

2.1. Compressive Properties of PEG Expanders

One of the key properties of a tissue expander is the mechanical strength, to guarantee dimensional stability in vitro and in vivo.[2,25] The mechanical properties of the engineered PEGDA-based expanders were evaluated in compression mode. Stress–strain curves and compressive modulus of the expander samples are shown in Figure 1A,B, respectively. If the soft tissue expanders are either too stiff (small elongation) or too soft (with relatively low strength), the mechanical properties would not be compatible with natural tissues.[38] The mechanical testing results showed that monomer combinations resulted in a variety of hydrogels with low to high moduli. For example, expanders comprised solely of the short-chained PEGDA-2k (sample P1) had compressive modulus around 145 ± 26.9 kPa, which was much higher than the modulus of the soft tissues (8–17 kPa).[39] In addition, it had low compressive strain at break (32 ± 5.6%) as compared to soft and elastic tissues. In contrast, expanders comprised solely of the long-chained PEGDA-10k (sample P3) had the compressive modulus around 13.3 ± 0.3 kPa with limited compressive strength; therefore, it may collapse in vivo.

We also found that by changing the ratio of the low to high molecular weight components in a polymer blend, it is possible to control the mechanical properties of the expanders with acceptable compressive modulus, compressive strength, and high strain at break while retaining other physical properties such as swelling behavior in an acceptable range. As shown in Figure 1A,B, P2 hydrogel (PEGDA-6k) showed compression strength and compressive modulus of 217.6 ± 51.4 kPa and 110 ± 20.5 kPa, respectively, with 60.5 ± 0.7% strain

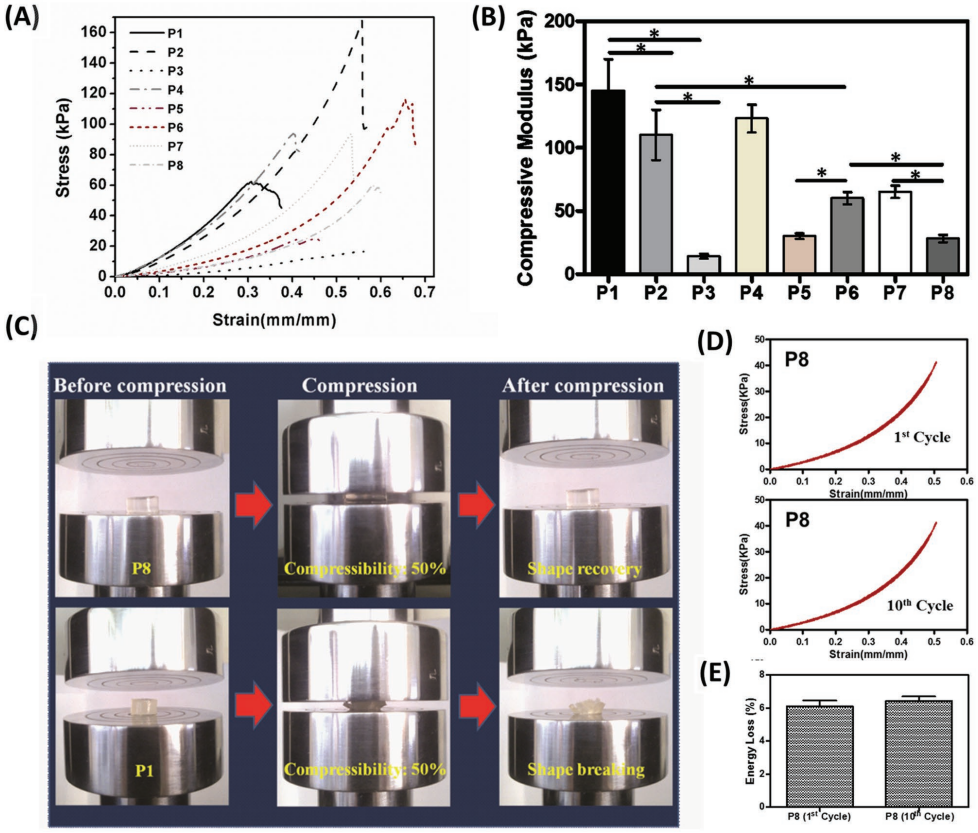

Figure 1. Mechanical properties of PEGDA-based hydrogel expanders. A) Representative stress–strain curves of the hydrogels, B) compressive moduli of expanders, C) P1 and P8 samples before compression, at 50% compression, and after compression. D) Representative compressive cyclic loading and unloading curves for P8 expanders at cycles 1 and 10 and E) energy loss calculated from the area between the loading and unloading curves of P8 gels based on cycles 1 and 10 (*$p < 0.05$). The error bars represent standard deviation (SD).

at break, while for the P8 hydrogel (blend of PEGDA-6k and PEGDA-10k), lower compression strength (73.4 ± 13.1 kPa), compressive modulus (28.3 ± 1.5 kPa), and strain at break (62 ± 1.5%) were obtained. Therefore, through this blending strategy it is feasible to engineer materials with tunable modulus of elasticity to be much closer to the soft tissue. With increasing the concentration of PEGDA with higher molecular weight in the blend, the rigidity of hydrogel was reduced as observed from the compressive moduli values reported in Figure 1B. P6 and P8 hydrogels may have sufficient compressive modulus and strength, preventing the collapse of self-inflating hydrogel. The lower compressive modulus of P5 sample might be due to the large differences between molecular weights of the blend components (large differences between the molecular weights of PEGDA-2k and PEGDA-10k) as opposed to P6 composite with more uniformly component's molecular weights ($p < 0.05$). It is hypothesized that in the P5 composite hydrogel, short-chained component (PEGDA-2k) behaved like site of cross-linking between the components of longer chained (PEGDA-10k). Samples P4 and P5 with poor mechanical properties among blend compositions (Table S1, Supporting Information), including low compressive strain at break (<0.5 mm mm^{-1}), were of limited practical use as they may result in fracture and, therefore, these samples were not subjected to further studies.

Previous studies have reported the effects of PEGDA polymer chains length on mechanical properties of the resulting hydrogels. For example, Zellander et al. showed that combinations of short and long PEGDA chains created polymer structures with increased strength and stiffness compared to structures composed of a given longer PEGDA chain.[40] Lin et al. also demonstrated that varying the molecular weight of PEGDA precursors exhibited a significant effect on the structural and mechanical properties of the hydrogels.[38] Mazzoccoli et al. have reported that different ratios of PEGDA chain sizes resulted in different stiffness or elastic modulus values, which affected cell viability.[41] Myung et al. also used PEG chains ranging from 3.4 to 14 kg mol^{-1} to adjust the mechanical properties of interpenetrating polymer networks composed of PEG and poly (acrylic acid).[42]

Shape retention/deformation of the P1 and P8 hydrogels are compared under compression (before

compression, at 50% compression and after load release at the end of compression test) in Figure 1C. The presence of longer polymer chains in P8 hydrogel caused increased chain mobility during mechanical deformation and facilitated the shape recovery processes. Moreover, the ability of P8 hydrogel to withstand mechanical loading and unloading was studied by performing cyclic compression at 50% strain. The results showed that this sample was capable of withstanding at least ten cyclic mechanical loading and unloading without crack formation and significant permanent deformation. As shown in Figure 1D,E, P8 hydrogel deformed reversibly following ten cycles of loading and unloading (see Figure S1 in the Supporting Information for P1). Energy loss based on cycles 1 and 10 was found to be 6.1 ± 0.6% and 6.4 ± 0.4% for P8 samples. An elastic network is fully recoverable to its original dimension under compression or elongation.[25] Due to ability to withstand several cycles of loading and unloading with a low energy loss (6%), P8 sample can be considered as an elastic material. The flexible and elastomeric nature of these networks can be partially attributed to the sufficiently long and flexible PEGDA chains between cross-links. Overall, adjusting PEGDA chain lengths is an efficient method for modulating the mechanical properties of PEGDA-based tissue expanders. The proportion of the PEGDA-2k, PEGDA-6k, and PEGDA-10k in the hydrogels may be varied depending on the desired clinical requirements.

2.2. Pore Characteristics and Swelling Ratio of PEGDA Expanders

Figure 2A summarizes representative scanning electron microscopy (SEM) images of selected expanders, at fractured surfaces of freeze-dried hydrogels. All the hydrogel samples showed highly interconnected porous structures. The apparent pore size of the hydrogels with different compositions was quantified by Image J software based on the SEM images from 20 randomly selected pores per image. The mean ± SD was used to interpret the data (Figure 2B). As anticipated, pore size and porosity strongly depended on the hydrogel compositions and correlated with the precursor molecular weight. For example, PEGDA-2k hydrogel (sample P1) demonstrated apparent pore size and porosity of 3.75 ± 0.86 μm and 70 ± 0.5%, respectively, while for the P8 hydrogel, higher apparent pore size (30.54 ± 8 μm) and porosity (82.8 ± 0.43%) were obtained. Although we observed some differences in the porosity of the engineered hydrogels, it is important to note that the pore structures of freeze-dried samples may be different as compared to hydrogel network in hydrated state due to the lyophilization process.

One important property that may be used for the characterization of expanders is the difference between their dry and wet masses. The hydration properties of the prepared hydrogels were evaluated by submerging the samples in saline solution (0.9%) at physiological temperature (37 ± 1 °C). As shown in Figure 2D,E, a high degree of hydration was observed for PEG-based hydrogels when exposed to an aqueous environment due to the hydrophilic nature of PEGDA. As anticipated, the equilibrium swelling was found to be dependent on the corresponding PEG's molecular weight; the mass swelling ratio increased with PEGDA molecular weight (Figure 2D). For example, P8 hydrogel demonstrated mass and volume equilibrium swelling of 1054 ± 23% and 1091 ± 88% after 7 d, respectively, while for the tightly cross-linked P1 hydrogel, lower mass (455 ± 35%) and volume (514 ± 20%) equilibrium swelling were obtained. Similar results were reported earlier in the literature for PEGDA hydrogels based on precursors of varying molecular weights.[38] Overall, with increase of the molecular weight or the content of higher molecular weight PEGDA in the compositions, the hydrophilicity of the polymer gels and hence the swelling can increase. In conclusion, our swelling studies clearly indicated that P6 and P8 expanders displayed a marked tendency to swell and are the most appropriate tissue expander candidates with outstanding expansion ability.

2.3. Network Properties of PEGDA Hydrogels

Success of these mixed PEGDA hydrogels as tissue expander may be governed by the mechanism of water diffusion. Water absorption process involves diffusion of water molecules into the free spaces, which leads to expansion of chain segments between cross-links and results in swelling. Using Equation (5), "k" and "n" were evaluated from the plots of "ln S_t" versus "ln t" as is shown in Figure 3A. All of the tested expanders gave an "n" value of ≈0.5 indicating Fickian diffusion in these gels.[5] So, Equation (5) may be simplified to

$$\frac{S_t}{S_\infty} = 4\left(\frac{Dt}{\pi L_o^2}\right)^{\frac{1}{2}} = Kt^{\frac{1}{2}} \quad (1)$$

The diffusion coefficient for water was determined by plotting $\frac{S_t}{S_\infty}$ against $\frac{t^{1/2}}{L_o}$ (see Figure 3B and Table S2, Supporting Information). For saline solution, D values of $(5.85 \pm 0.2) \times 10^{-7}$ and $(1.35 \pm 0.14) \times 10^{-7}$ m^2 s^{-1} were calculated for the P1 and P8 hydrogels, respectively. In general, the lower the molecular weight of the polymer chain, the higher the diffusion of the solute. Similar strategies have been used to determine the diffusion coefficient for water in self-inflating tissue expanders. For example, Swan et al. showed that distilled water has D values of

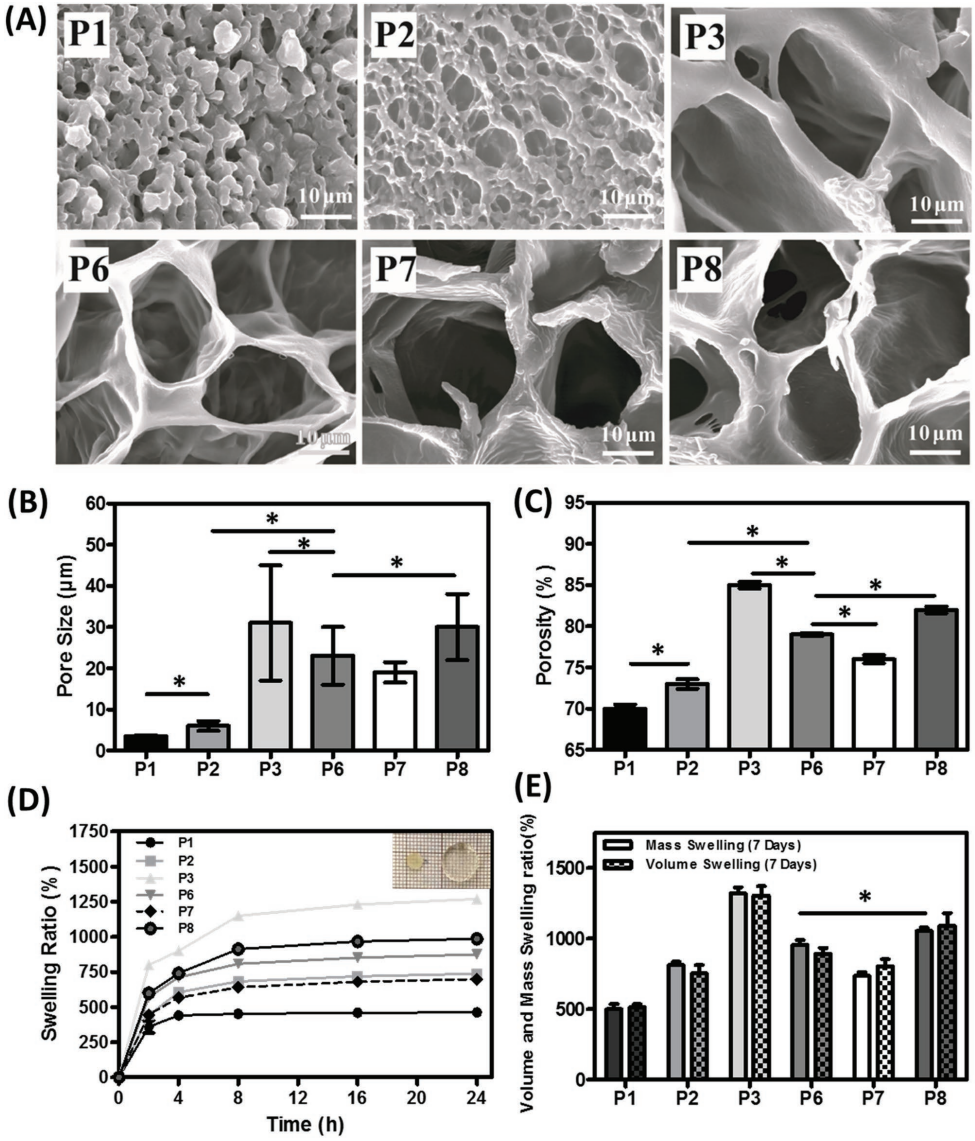

Figure 2. A) SEM images from the cross-sections of the engineered PEGDA hydrogels with varying compositions, showing highly interconnected and porous structures for all formulations. B) The apparent pore size of the hydrogels with different compositions quantified by Image J software based on the SEM images. C) Porosity at equilibrium. D) Mass swelling ratio after 24 h incubation in saline solution. The mass swelling ratio increased with the PEG molecular weight. E) Volume and mass swelling equilibrium after 7 d (*$p < 0.05$). The error bars represent standard deviation (SD).

$(1.63 \pm 0.29) \times 10^{-7}$ and $(0.35 \pm 0.04) \times 10^{-7}$ m^2 s^{-1} for two types of VP/MMA hydrogel tissue expanders.[5]

The swelling ratio of expanders depends on the hydrophilic ability of the polymer gel, the cross-linking density, and free space in the network of the hydrogel.[43] Generally, the hydrogel with higher network space (or mesh size) and lower cross-linking density are capable to adsorb larger amounts of water.[2] Assuming the hydrogel behaves like an elastic network, effective cross-linking density is determined from Equation (6). A comparison of the results showed that the determined cross-linking density in low molecular weight samples was higher than that in high molecular weight ones (Figure 3C and Table S2, Supporting Information). On the other hand, the average molecular weight between cross-links ($\overline{Mc}$) increased from 450.9 ± 20.3 g mol^{-1} for P1 to 1724.6 ± 27.9 g mol^{-1} for P8 (Figure 3D and Table S2, Supporting Information). Mesh size calculations showed a similar trend and an increase from 2.58 ± 0.08 nm for P1 to 5.99 ± 0.35 nm for P8. As shown in Figure 3D, presence of long chain precursors in the network resulted in significantly larger mesh size and increased molecular weight between cross-links. Similar results were reported by Lin et al., who showed that the structural properties of the PEGDA hydrogels could be controlled by varying the molecular weight of PEGDA precursors.[38]

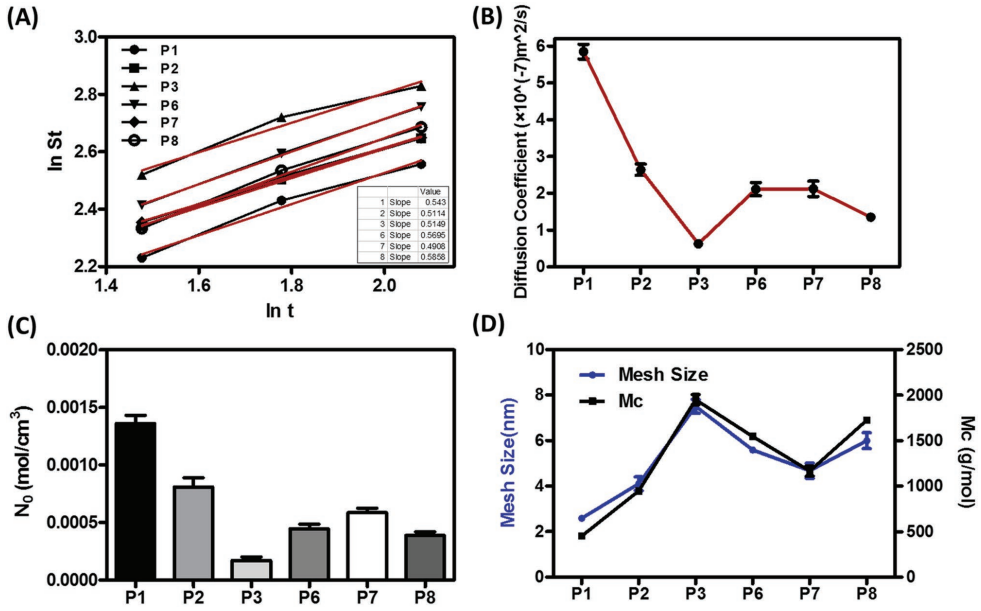

Figure 3. Network characterization of hydrogels. A) Plots of "ln S_t" versus "ln t". All of the tested expanders gave an "n" value of ≈0.5 indicating Fickian diffusion through the gels. B) Diffusion coefficient for water; presence of long chains in the compositions reduced the diffusion of solute. C) Cross-linking density for each composition. Cross-linking density in low molecular weight samples is higher than other compositions . D) Average molecular weight between cross-links ($\overline{Mc}$) and mesh size for each composition. The error bars represent standard deviation (SD).

The conclusion can be drawn that, of the eight studied compositions, P6 and P8 hydrogels with the described mechanical properties and outstanding swelling ratios are potential expander candidates. The P6 and P8 hydrogels provided a balance of mechanical property and swelling capability.

2.4. In Vitro Cytocompatibility Tests

Before in vivo experiments, cytotoxicity of the hydrogels was evaluated qualitatively in vitro by a direct method according to ISO 10933, using L929 fibroblasts as model cell line. Optical microscopy showed that cells possess normal morphology after 48 h of seeding (Figure S2, Supporting Information).

2.5. PEG Hydrogels as Expanders: In Vivo Study

2.5.1. Tissue Expansion

To assess the capability of these newly developed blend expanders in generation of sufficient pressure to dilate the surrounding tissue, selected samples were implanted subcutaneously in rats for 4 and 21 d. The study comprised six male Wistar rats. The six rats were divided into two groups: group 1 with three rats for 4 d study and group 2 with three rats for 21 d study. P6 and P8 hydrogels, which exhibited the most promising in vitro mechanical and swelling characteristics, were selected for the in vivo tests. As shown in Figure 4A, in each rat two expanders (one P6 and one P8) were implanted.

We found that the swelling pressure of both P6 and P8 expanders could overcome the resistance of the adjacent tissues and led to a considerable dilation. Figure 4A shows the ability of the implanted hydrogels to expand in vivo after 21 d of subcutaneous implantation. An increase in the size of the expanders was already obvious in the first few days. Throughout the first week of the observation period, this process resulted in a considerable expansion of the skin. After 21 d, macroscopically, the expanded skin in all the groups was in excellent shape with normal hair growth on it and there was no difference in the texture of expanded and normal skin (Figure 4A). Based on previous studies, soft tissue optimization by pretreatment with self-inflating tissue expanders reduces the incidences of postoperative wound dehiscence in complex augmentation surgeries.[44,45] There was no sign of complications reported for previous expanders in the literature such as necrosis, perforation, infection, and wound separation.[9,46] During the postoperative period, no sign of pain was observed and all the wounds healed completely without complications.

Figure 4B(I),C(I) shows representative images of the expanded skin and the fibrous capsule developed around the expanders at both time points. Within days after placement of the tissue expanders, a new network of vessels developed as can be observed in Figure 4B(II),C(II). An ideal tissue expander should

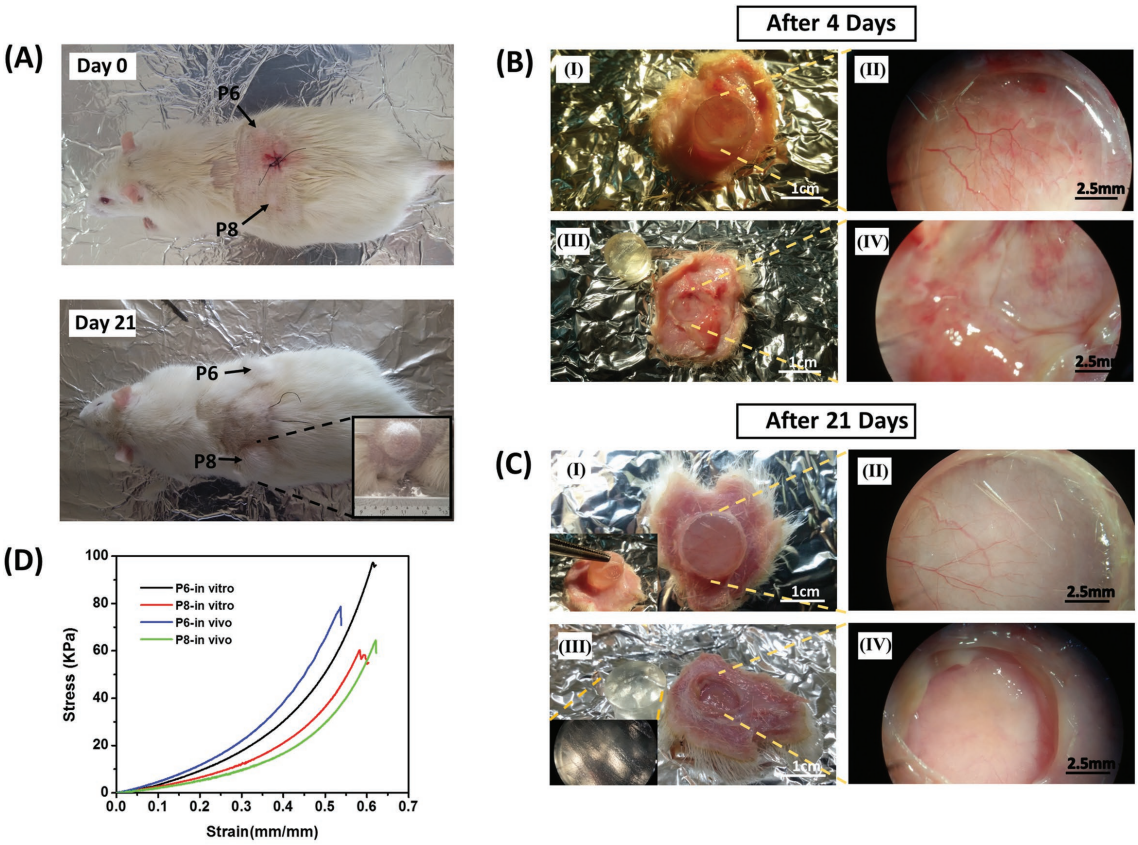

(E)

	Sample	Compressive Modulus (KPa)	Compressive Strain at break (mm/mm)	Compressive Strength (KPa)	Mass Swelling ratio (%)	Volume Swelling ratio (%)
After 4 days	P6	65.7±5.6	0.53±0.04	98.1±6.3	888.3±5.7	903.4±22.3
	P8	32.6±3.4	0.55±0.037	80.4±7.2	992.3±34.4	1029±54.9
After 21 days	P6	58.9±4.9	0.53±0.06	93.2±10.1	923.9±28.4	953.6±36.8
	P8	27.3±5.6	0.62±0.058	64.5±5.7	1102.9±50.3	1108±61.9

Figure 4. In vivo studies on engineered PEGDA expanders. A) Day 0: two expanders (one P6 and one P8) were implanted in each rat. Day 21: Both expanders generated enough swelling pressure to dilate the adjacent tissue. In addition, the expanded skin in all groups was in excellent shape with normal hair growth on it. B) In vivo study 4 d after subcutaneous implantation (sample P8). (I) The explanted area includes the expanded skin and the developed granulation tissue that completely surrounded the expanders. (II) Magnification of granulation tissue with blood vessels under loop microscope. (III) The expander was removed from the overlying expanded skin and granulation tissue. The hydrogel retained its original shape after explantation. (IV) Magnification of the expanded skin under loop microscope demonstrated signs of mild inflammation (between 10% and 30%). C) In vivo study 21 d after subcutaneous implantation (sample P8). (I) The expanded skin and the developed fibrous capsule completely surrounded the expanders. (II) Magnification of fibrous capsule with blood vessels under loop microscope. (III) The expander was removed from the overlying expanded skin and fibrous capsule. The expander device retained its original shape after explantation. (IV) Magnification of the skin on the site of expansion with the aid of loop microscope demonstrated no sign of inflammation (less than 10%). D) Representative stress–strain curves of P6 and P8 hydrogels before and after implantation (day 21) both in the swollen state. E) Mechanical and swelling properties of explanted hydrogels on both postoperative days 4 and 21.

retain its shape upon implantation and during the explantation phase.[11] After explantation, both P6 and P8 expanders showed considerable swelling ratio while retaining their original shapes (Figure 4B(III),C(III)). Expanded skins on the site of expansion are shown with the aid of loop microscope in Figure 4B(IV),C(IV). On postoperative day 4 (Figure 4B(IV)), there were signs of slight inflammation.

2.5.2. Mechanical Properties and Swelling Behavior of Expanders after Explantation

The mechanical and swelling properties of both groups were obtained after explantation (Figure 4D,E). The results for compression test indicated that the compressive modulus and strength of the explanted hydrogels were not significantly different compared to the samples

swelled in saline solution in vitro ($p > 0.05$). Data shown in Figure 4E confirmed that the swelling ability was lower but still significant under in vivo circumstances (the hydrogels expanded around ten times their initial volume) as compared to other osmotic hydrogel expanders consisted of a copolymer based on methyl methacrylate and vinyl pyrrolidone (two to four times).[1,4] Previous publications have also reported that the swelling expansion of the device in vivo is similar to swelling ratio in physiological phosphate buffered saline (PBS) solution in vitro.[47]

2.5.3. Histology

As shown in Figure 5A,B, 4 d following implantation of the expanders, granulation tissue was formed with its characteristic histological features including the proliferation of new blood vessels and fibroblasts. These connective tissue capsules demonstrated different levels of vascularization, depending on the expander volume.[22] No giant cells were observed. Light microscopy revealed a slight to moderate accumulation of macrophages in the expanded skin biopsies in group 1. They demonstrated signs of mild inflammation (between 10% and 30%).

After 3 weeks of implantation, the preliminary histological analysis results (Figure 5C,D) revealed the formation of fibrous capsule and significant vessel proliferation at the interface between the implant and the subcutaneous tissue as the tissue reacts to a foreign body. In accordance with our findings, the same histological structure of the fibrous capsule was also described by Von See et al. for VP/MMA expanders.[22] They demonstrated signs of slight inflammation (less than 10%) for P6 and signs of mild inflammation (between 10% and 30%) for P8. No giant cells could be observed. Additionally, there were no eosinophils present after 21 d for both P6 and P8 expanders.

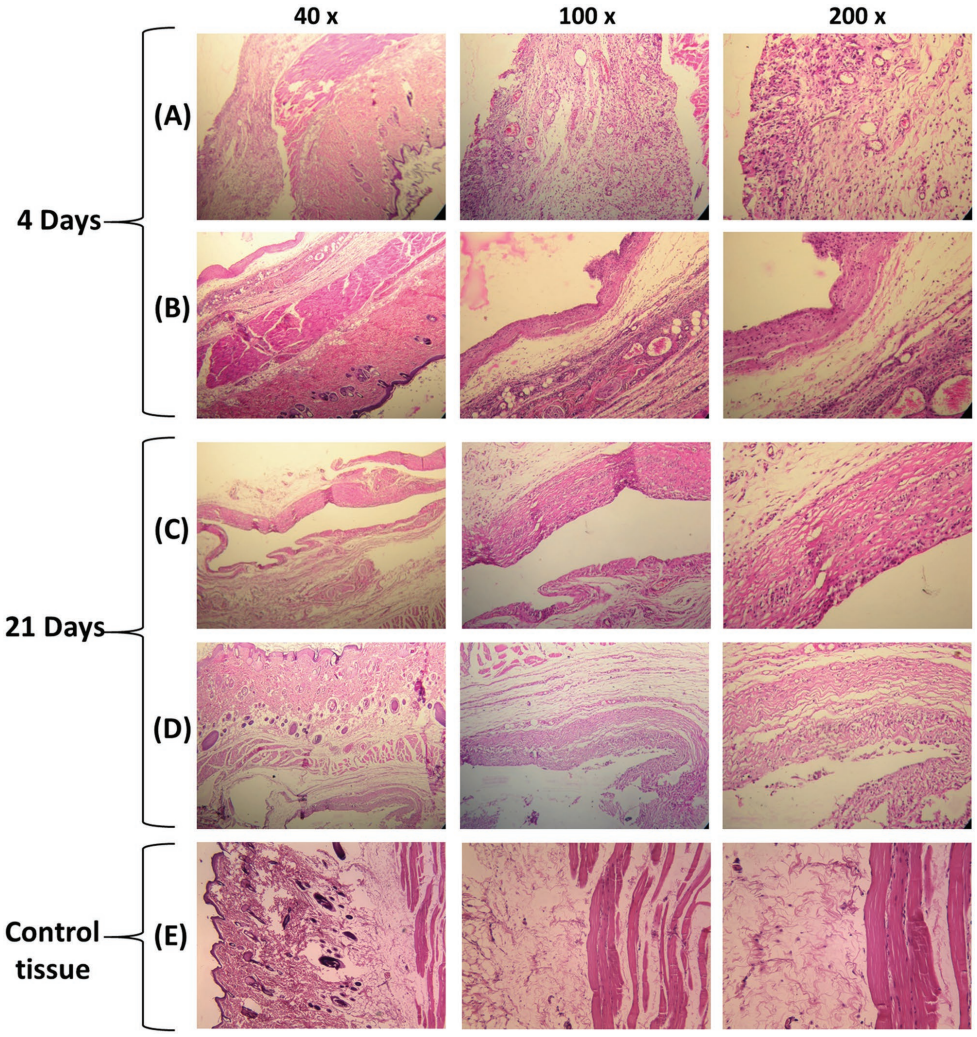

Figure 5. Hematoxylin eosin staining of subcutaneously implanted PEGDA expanders and control tissue in three different magnifications. A) P6 and B) P8 on postoperative day 4 (group 1). C) P6 and D) P8 on postoperative day 21 (group 2). E) Control tissue.

Previous studies have also reported the histological features of tissue samples taken at the end of expansion period. For example, Varga et al.[11] showed that in 50% of the animals that received the acrylic acid expander, ulceration of the skin and for acrylamide expanders a slight to moderate accumulation of macrophages in the expanded skin biopsies were observed on postoperative day 18. Their results demonstrated that with the use of NIPAAm polymers, the overlying skin did not show pathological changes.

A tissue compatible material shows a normal inflammatory reaction and is surrounded by a thin, uniform fibrous capsule in which multinucleated giant cells and other inflammatory cells are generally absent.[48] Concerning this definition, these expanders investigated in this study appear biocompatible as confirmed by other previously reported investigations on other applications of the same basic material.[28]

3. Conclusion

In this study, highly resilient, self-inflating expanding hydrogels based on PEGDA polymers with different molecular weights were developed. We synthesized a library of PEG-based expander hydrogels, which were resilient and had tunable mechanical properties and swelling behavior, along with an easy method of fabrication. It was found that by changing the ratio of the low to high molecular weight components in the polymer blend, it is feasible to design versatile composition formulations depending on the desired clinical requirements of the site of expansion. For this study, of the eight studied compositions, P8 hydrogel with described mechanical properties and significant swelling ratio shows potential to be used as a tissue expander. In vivo examination revealed that the selected expander was able to generate sufficient swelling pressure to expand skin and at the same time swell considerably while retaining its original shape after explantation. Collectively, these results suggest that while avoiding vigorous synthesis conditions, our mechanically tunable and resilient PEG-based hydrogels have potential to be developed as self-inflating matrices for engineering a variety of tissue expanders.

4. Experimental Section

4.1. Materials

PEG polymers with molecular weights (M_ws) of 2, 6, and 10 kDa were purchased from Merck. Ac and triethylamine were purchased from Sigma-Aldrich. Dimethyl sulfoxide (DMSO), benzene, and diethyl ether were obtained from Merck. 2,2-Azobisisobutyronitrile (AIBN) as a radical initiator was purchased from Sigma-Aldrich and used after recrystallization in methanol. Other chemicals were used as received.

4.2. Synthesis of PEGDA Precursors

PEGDA was synthesized through reaction between acryloyl chloride and hydroxyl end groups of PEG based on the previously explained procedure with minor modifications.[27] Dry PEG (20 g) was conveyed to a round bottom flask and fourfold molar excess triethylamine was added drop wise while stirring. A four-fold molar excess of acryloyl chloride was added drop wise to this reactant mixture in an ice bath. The reaction was stirred at 80 °C for 3 h under nitrogen followed by stirring at room temperature for 2 h. The reacted mixture was then filtered to remove triethylamine hydrochloride. The filtrate was condensed on a rotary evaporator and precipitated in diethyl ether. Precipitated products were re-dissolved in benzene and re-precipitated in diethyl ether (three times). Finally, the precipitated PEG diacrylates were dried at 40 °C under reduced pressure for 24 h. PEGDA with molecular weights of 2 kDa (PEGDA-2k), 6 kDa (PEGDA-6k), and 10 kDa (PEGDA-10k) were prepared using the same procedures. The acrylation degree of PEGDA was more than 65% as quantified by 400 Hz ^{1}H nuclear magnetic resonance on a BrukerARX400 spectrometer.

4.3. Preparation of PEGDA Hydrogels

PEGDA polymers with different molecular weights were used at different feed ratios to make various hydrogels. The prepared diacrylates (15 wt%) were dissolved in DMSO. Once the PEGDA polymer was dissolved, an initiator solution composed of AIBN dissolved in DMSO was added to the PEGDA/DMSO solution. For every precursor solution, the final concentration of the initiator was 0.5 wt%. The mixtures were then subjected to ultracentrifugation (10 000 rpm for 10 min) to remove air bubbles. The hydrogels were then formed in a drying oven at 60 °C for 24 h. After gel formation, both ends of the Eppendorf tubes were cut and the hydrogels were pulled out. The hydrogels were cut and placed in distilled water for 2–3 d. The distilled water was periodically changed to remove any potential residual monomers or polymers, followed by drying in a vacuum oven at room temperature for 2–3 d.

4.4. Compression Tests

According to ASTM F2900, the compression testing can be performed for sufficiently robust hydrogels under static conditions and in unconstrained geometries. The compressive modulus, compressive strength, and strain at break of the engineered hydrogels were measured in their equilibrium-swollen state by using a Universal Testing system (STM-20, SANTAM, Iran). Cylindrical gels with the height of about 5 mm and diameter of 8 mm were prepared. A force load of 60 N and a crosshead speed of 1 mm min^{-1} were employed. The compressive moduli of the gels were calculated as the slope of the linear region of the stress–strain curves, between 0.05 and 0.2 mm mm^{-1} strain. The ability of hydrogels to withstand mechanical loading was studied by cyclic compression tests (ten cycles) performed at a strain level of

50%. The average and standard deviation of values were obtained for three samples.

4.5. Scanning Electron Microscopy

The pore morphology of the hydrogels was observed using a scanning electron microscope (SEM) (ATS2100, Seron Technology, Korea). The swollen hydrogels were frozen with liquid nitrogen and fractured. The samples were then lyophilized and sputter-coated with gold for SEM analysis. The apparent pore sizes (average pore diameter) were calculated as the mean diameter of the pores observed from SEM images and quantified by using Image J software. Three images were taken from different parts of three different samples and pores were manually selected per image for pore sizing ($N = 20$).

4.6. Swelling Behavior

The swelling behaviors of hydrogels were measured in 0.9% saline solution. All experiments were conducted at 37 ± 1 °C, and the tests were continued until an equilibrium-swelling ratio ($S\infty$) was obtained. The hydrogels were taken out from the solution at periodic intervals of time and their masses at the time (M_t) were measured after gently removing surface water with filter paper. Each experiment was repeated three times per sample type. The swelling behavior (S_t) was calculated based on the changes in the mass as a function of time using Equation (2)[49]

$$S_t = \left[\frac{M_t - M_d}{M_d}\right] \tag{2}$$

where M_t and M_d represent the mass of the hydrogel at time t and the xerogel (lyophilized hydrogels), respectively.

4.7. Porosity

A liquid displacement method was used to measure the porosity.[50] Dried samples were immersed in distilled water overnight and weighed after removing the excess water on the hydrogel surfaces. The porosity was determined using Equation (3)

$$\text{porosity} = \frac{M_2 - M_1}{\rho V} \tag{3}$$

where M_1 and M_2 are the mass of the gel before and after immersion in water; ρ is the density of the water and V is the volume of the gel.

4.8. Diffusion Coefficient

Equation (4) can be used to calculate the diffusion coefficient (D) for a xerogel disk of initial thickness (L_0), swelled in a solvent under constant boundary conditions[5]

$$\frac{S_t}{S_\infty} = 1 - \sum_{n=0}^{\infty} \left(8/(2n+1)^2\pi^2\right) \exp\left[-(2n+1)^2\pi^2\left(4Dt/l_0^2\right)\right] \tag{4}$$

Consequently, at early times of the process, when $\frac{S_t}{S_\infty} \leq 0.6$,[5] Equation (4) may be simplified to Equation (5)

$$\frac{S_t}{S_\infty} = 4\left(\frac{Dt}{\pi L_0^2}\right)^n = Kt^n \tag{5}$$

where K is a swelling constant; and n is the swelling exponent, indicating the water transport mechanism.

4.9. Cross-Linking Density

Effective cross-linking density (N_0) was calculated using Equation (6)[5,51,52] (see the Supporting Information)

$$N_o = \frac{\rho}{\overline{M_c}}\left(1 - \frac{2\overline{M_c}}{\overline{M_n}}\right) \tag{6}$$

where $\overline{Mn}$ is the average molecular weight of PEG oligomers and ρ is the polymer density.

4.10. Mesh Size

The equilibrium swelling of the cross-linked hydrogels was in part governed by the cross-linking density and was estimated from the molecular weight between cross-links (Mc).[9] The average molecular weight between cross-links ($\overline{Mc}$) and the mesh size (ξ) of the hydrogel was calculated according to the Peppas and Merrill model[51,38] (see the Supporting Information).

4.11. In Vitro Cytotoxicity Studies

The in vitro cytotoxicity of the gels was evaluated by using a direct contact method according to ISO 10933.[53] The hydrogel samples were cut into 100 μm thickness disks with vibroslicer (752M Vibroslice, Campden Instruments, UK). Subsequently, the hydrogels were sterilized in 70% ethanol followed by washing with sterile PBS for 2 d and placing under UV radiation for 30 min. The properties of PEG-based hydrogels did not change by applying UV radiation for the purpose of hydrogel sterilization.[25] The sterilized hydrogels were placed individually into each well of an ultralow attachment 12 well plates. Before seeding the cells on the gels, samples were hydrated in the media for 2 h. Tissue culture polystyrene surface was used as a positive control. L929 fibroblast cell lines (1 mL) were added into each well (final cell density: 1×10^5 cells well^{-1}) and incubated at 37 °C with the hydrogel samples. The culture medium composed of Roswell Park Memorial Institute (RPMI) 1640 medium with 10% fetal bovine serum and 1% penicillin/streptomycin. After 48 h, cell morphology was observed and images were taken using inverted compound microscopy (Eclipse TE2000-U, Nikon, Spain).

4.12. Animal Experiments

Animal experiments were performed to evaluate the biocompatibility of the engineered hydrogels and to test their expansion capability in vivo. The experiments were performed on male Wistar rats (250 ± 25 g). All interventions were in accordance with the Declaration of Helsinki. The applied protocols were accepted by the Ethical Committee for the Protection of Animals in Scientific Research at the National Institute of Genetic Engineering

and Biotechnology (NIGEB). The animals were anaesthetized with ketamine and xylazine (35–40 mg kg^{-1}, 0.2 mg kg^{-1}).

4.13. Subcutaneous Implants

For subcutaneous implantation, the hair of the dorsal region was removed and then a skin incision was made. Small pockets were created between the dorsal fascia and the panniculus muscle using a blunt preparation. The hydrogels, which exhibited the most promising mechanical and swelling characteristics in vitro, were chosen for in vivo observations. Cylindrical gels were formed with a diameter and length of ≈5 and 3 mm, respectively. Prior to the implantation, the dry masses (M_d) of the samples were measured. The samples were placed into the pockets and the wound areas were closed with simple interrupted sutures. The animals received no antibiotics. On postoperative days 4 and 21, the animals were sacrificed followed by explantation of the expander samples including the adjacent tissue. The wet mass (M_t) of the expanders was measured immediately and the swelling ratios were calculated. Afterward, the samples were processed for histological analyses and compressive mechanical studies.

4.14. Histology

For histological analysis the samples were fixed for 24 h in 5% formaldehyde (pH 7.4) and rinsed in water. Then, they were decalcified in 10% Ethylenediaminetetraacetic acid (EDTA) (in 0.3 M Tris HCl pH 7.4) and paraffin embedded before sectioned in 5 μm intervals. The sections were stained based on standard protocols with hematoxylin eosin.

4.15. Statistical Analysis

The experiments were performed at least in triplicate. The results were reported as means ± standard deviation. The statistical differences were determined by analysis of variance followed by Student's *t*-test. Results were considered statistically significant when $p < 0.05$.

Supporting Information

Supporting Information is available from the Wiley Online Library or from the author.

Acknowledgements: The authors wish to acknowledge financial support provided for this work by the National Institute of Genetic Engineering and Biotechnology (NIGEB). A.K. also acknowledges funding from the National Institutes of Health (AR057837, DE021468, D005865, AR068258, AR066193, EB022403, and EB021148) and the Office of Naval Research Presidential Early Career Award for Scientists and Engineers (PECASE). B.H. acknowledges the support from the Research Administration of Shahid Beheshti University of Medical Science. N.A. acknowledges the support from the American Heart Association (AHA, 16SDG31280010) and FY17 TIER 1 Interdisciplinary Research Seed Grants from Northeastern University. The authors gratefully acknowledge the scientific help and guidance of Mohammad Atai and Alireza Hassani Najafabadi.

Received: November 14, 2016; Revised: January 30, 2017; Published online: April 6, 2017; DOI: 10.1002/mabi.201600479

Keywords: hydrogel; mechanical properties; poly (ethylene glycol) diacrylate; swelling behavior; tissue expander

[1] H. J. Uijlenbroek, Y. Liu, J. F. He, C. Visscher, M. A. van Waas, D. Wismeyer, *Clin. Oral Implants Res.* **2011**, *22*, 121.
[2] T. H. Tran, J. Garner, Y. Fu, K. Park, K. M. Huh, *Handbook of Biodegradable Polymers: Isolation, Synthesis, Characterization and Applications*, Wiley, Teltow, Germany **2011**.
[3] A. Fochtmann, M. Keck, M. Mittlböck, T. Rath, *Burns* **2013**, *39*, 984.
[4] C. Von See, M. Rücker, K.-H. Bormann, N.-C. Gellrich, *Br. J. Oral Maxillofac. Surg.* **2010**, *48*, e5.
[5] M. Swan, D. Bucknall, T. Goodacre, J. Czernuszka, *Acta Biomater.* **2011**, *7*, 1126.
[6] C. G. Neumann, *Plast. Reconstr. Surg.* **1957**, *19*, 124.
[7] a) C. Radovan, *Plast. Reconstr. Surg.* **1982**, *69*, 195; b) C. Radovan, *Plast. Reconstr. Surg.* **1984**, *74*, 482.
[8] L. C. Argenta, M. W. Marks, W. C. Grabb, *Ann. Plast. Surg.* **1983**, *11*, 188.
[9] D. Bucknall, J. Czernuszk, J. Lee, Z. Radzi, M. Swan, *US20120265165*, **2010**.
[10] K. A. Hurvitz, H. Rosen, J. G. Meara, *Int. J. Pediatr. Otorhinolaryngol.* **2005**, *69*, 1509.
[11] J. Varga, L. Janovak, E. Varga, G. Eros, I. Dekany, L. Kemeny, *Skin Pharmacol. Physiol.* **2009**, *22*, 305.
[12] E. D. Austad, G. L. Rose, *Plast. Reconstr. Surg.* **1982**, *70*, 588.
[13] K. Wiese, *J. Craniomaxillofac. Surg.* **1993**, *21*, 309.
[14] M. Akbari, A. Tamayol, S. Bagherifard, L. Serex, P. Mostafalu, N. Faramarzi, M. H. Mohammadi, A. Khademhosseini, *Adv. Healthcare Mater.* **2016**, *5*, 752.
[15] K. Wiese, D. Heinemann, D. Ostermeier, J. Peters, *J. Biomed. Mater. Res.* **2001**, *54*, 179.
[16] S. R. Shin, S. M. Jung, M. Zalabany, K. Kim, P. Zorlutuna, S. b. Kim, M. Nikkhah, M. Khabiry, M. Azize, J. Kong, *ACS Nano* **2013**, *7*, 2369.
[17] G. C. Ingavle, S. H. Gehrke, M. S. Detamore, *Biomaterials* **2014**, *35*, 3558.
[18] X. Zhao, *Soft Matter* **2014**, *10*, 672.
[19] R. Downes, M. Lavin, R. Collin, *Adv. Ophthal. Plast. Reconstr. Surg.* **1991**, *9*, 57.
[20] K. F. Kobus, *J. Plast. Reconstr. Aesthet. Surg.* **2007**, *60*, 414.
[21] M. C. Swan, T. E. Goodacre, J. T. Czernuszka, D. G. Bucknall, *J. Plast. Reconstr. Aesthet. Surg.* **2008**, *61*, 220.
[22] C. Von See, N. C. Gellrich, U. Jachmann, M. W. Laschke, K. H. Bormann, M. Rücker, *Clin. Oral Implants Res.* **2010**, *21*, 842.
[23] Y. Zhu, J. T. Czernuszka, *J. Med. Bioeng.* **2015**, *4*, 87.
[24] L. Kemény, I. Dékány, J. Varga, L. Janovák, *US20100239672*, **2008**.
[25] A. K. Gaharwar, C. P. Rivera, C.-J. Wu, G. Schmidt, *Acta Biomater.* **2011**, *7*, 4139.
[26] V. Hagel, T. Haraszti, H. Boehm, *Biointerphases* **2013**, *8*, 36.
[27] S. J. Im, Y. M. Choi, E. Subramanyam, K. M. Huh, K. Park, *Macromol. Res.* **2007**, *15*, 363.
[28] M. Browning, S. Cereceres, P. Luong, E. Cosgriff-Hernandez, *J. Biomed. Mater. Res., Part A* **2014**, *102*, 4244.
[29] S. Nemir, H. N. Hayenga, J. L. West, *Biotechnol. Bioeng.* **2010**, *105*, 636.

[30] B. Ozcelik, A. Blencowe, J. Palmer, K. Ladewig, G. W. Stevens, K. M. Abberton, W. A. Morrison, G. G. Qiao, *Acta Biomater.* **2014**, *10*, 2769.
[31] S. H. Lee, B. S. Kim, S. H. Kim, S. W. Choi, S. I. Jeong, I. K. Kwon, S. W. Kang, J. Nikolovski, D. J. Mooney, Y. K. Han, *J. Biomed. Mater. Res., Part A* **2003**, *66*, 29.
[32] Y. Jung, S. H. Kim, H. J. You, S.-H. Kim, Y. Ha Kim, B. G. Min, *J. Biomater. Sci., Polym. Ed.* **2008**, *19*, 1073.
[33] C.-W. Chang, A. van Spreeuwel, C. Zhang, S. Varghese, *Soft Matter* **2010**, *6*, 5157.
[34] M. B. Browning, E. Cosgriff-Hernandez, *Biomacromolecules* **2012**, *13*, 779.
[35] Q. T. Nguyen, Y. Hwang, A. C. Chen, S. Varghese, R. L. Sah, *Biomaterials* **2012**, *33*, 6682.
[36] J. W. Gunn, S. D. Turner, B. K. Mann, *J. Biomed. Mater. Res., Part A* **2005**, *72*, 91.
[37] G. M. Cruise, D. S. Scharp, J. A. Hubbell, *Biomaterials* **1998**, *19*, 1287.
[38] S. Lin, N. Sangaj, T. Razafiarison, C. Zhang, S. Varghese, *Pharm. Res.* **2011**, *28*, 1422.
[39] S. R. Shin, H. Bae, J. M. Cha, J. Y. Mun, Y.-C. Chen, H. Tekin, H. Shin, S. Farshchi, M. R. Dokmeci, S. Tang, *ACS Nano* **2011**, *6*, 362.
[40] A. Zellander, A. Kadakia-Bhasin, M. Mahksous, M. Cho, *Adv. Biomed. Eng. Res.* **2013**, *1*, 9.
[41] J. P. Mazzoccoli, D. L. Feke, H. Baskaran, P. N. Pintauro, *J. Biomed. Mater. Res., Part A* **2010**, *93*, 558.
[42] D. Myung, W. Koh, J. Ko, Y. Hu, M. Carrasco, J. Noolandi, C. N. Ta, C. W. Frank, *Polymer* **2007**, *48*, 5376.
[43] S. Vural, K. B. Dikovics, D. M. Kalyon, *Soft Matter* **2010**, *6*, 3870.
[44] C. Mertens, O. Thiele, M. Engel, R. Seeberger, J. Hoffmann, K. Freier, *Clin. Implant Dent. Relat. Res.* **2015**, *17*, 44.
[45] D. Kaner, H. Zhao, W. Arnold, H. Terheyden, A. Friedmann, *Clin. Oral Implants Res.* **2016**, *1*, 1.
[46] S. Chummun, P. Addison, K. Stewart, *J. Plast. Reconstr. Aesthet. Surg.* **2010**, *63*, 2128.
[47] C. Stuehmer, M. Rücker, P. Schumann, K.-H. Bormann, Y. Harder, B. Sinikovic, N.-C. Gellrich, *J. Craniomaxillofac. Surg.* **2009**, *37*, 258.
[48] B. D. Ratner, A. S. Hoffman, *Hydrogels for Medical and Related Applications*, ACS, Washington, DC, USA **1976**.
[49] A. S. Sarvestani, W. Xu, X. He, E. Jabbari, *Polymer* **2007**, *48*, 7113.
[50] J. A. Killion, S. Kehoe, L. M. Geever, D. M. Devine, E. Sheehan, D. Boyd, C. L. Higginbotham, *Mater. Sci. Eng., C* **2013**, *33*, 4203.
[51] B. V. Slaughter, S. S. Khurshid, O. Z. Fisher, A. Khademhosseini, N. A. Peppas, *Adv. Mater.* **2009**, *21*, 3307.
[52] K. S. Anseth, C. N. Bowman, L. Brannon-Peppas, *Biomaterials* **1996**, *17*, 1647.
[53] M. Cheddadi, E. López-Cabarcos, K. Slowing, E. Barcia, A. Fernández-Carballido, *Int. J. Pharm.* **2011**, *413*, 126.